

# Thickness-related instability of Cu thin films on Ag(100)

M.A. Pfeifer<sup>a</sup>, O. Robach<sup>a</sup>, B.M. Ocko<sup>b</sup>, I.K. Robinson<sup>a,\*</sup>

<sup>a</sup>Department of Physics, University of Illinois, Loomis Laboratory of Physics, 1110 West Green Street, Urbana IL 61801, USA

<sup>b</sup>Physics Department, Brookhaven National Laboratory, Upton NY 11973, USA

## Abstract

Copper and silver have a sufficiently large mismatch of lattice parameters that the growth of Cu on Ag(100) substrates stabilizes the metastable body-centered cubic (BCC) form of Cu. This paper reports that layer-by-layer growth of the BCC film occurs up to a critical thickness of 10 ML, beyond which a structural instability arises in the thin film. This leads to a uniaxial laterally modulated phase giving rise to satellite peaks in the diffraction from both film and substrate. The characteristic dependence of satellite spacing versus film thickness is interpreted in terms of four possible variants of the modulated film structure. Only one of these variants is consistent with the observed growth behavior.

© 2004 Elsevier B.V. All rights reserved.

PACS: 61; 68.55.–a; 68.35.–p

Keywords: CuAg; Martensitic transformations; Surface buckling

## 1. Introduction

Crystalline matter is most stable when defects are avoided. Dislocations, which are the simplest extended defect in crystals, therefore feature centrally in the theories of thin film structure, such as that of Matthews and Blakeslee [1]. Because of mismatch at an interface between two crystals, a limited number of edge dislocations is

tolerated, with their energy cost offset by a reduction in elastic energy due to strain. Some systems, such as Cu thin films grown on Au(100) or Ag(100), avoid dislocations in a more radical way by adopting an altogether different crystal structure, in this case BCC in place of FCC. The energy saved by not forming dislocations exceeds the small energy penalty of the metastable BCC crystal form. This situation is expected to hold for thin films up to some critical thickness,  $h < h_C$ , beyond which the thicker films should revert to the normal FCC structure. This experimental study initially sought to observe the pathway followed by the films during this reversion process. By

\*Corresponding author. Tel.: +1 217 2442949;  
fax: +1 217 3336126.

E-mail addresses: [ben@solids.phy.bnl.gov](mailto:ben@solids.phy.bnl.gov) (B.M. Ocko),  
[ikr@uiuc.edu](mailto:ikr@uiuc.edu), [robinson@mrl.uiuc.edu](mailto:robinson@mrl.uiuc.edu) (I.K. Robinson).

analyzing the sequence of structures we expected to learn about the general relaxation mechanism of metallic films.

Previous investigations concerned the electrochemical Cu/Au deposition system [2,3]. Thin films, below 10 monolayers (ML) thick, were found to be in the metastable BCC state, lattice matched to the substrate with  $[1\ 1\ 0] \parallel [1\ 0\ 0]$ . These studies reported a transition in film thickness at 10 ML, above which the BCC cubic Cu film becomes unstable toward orthorhombic distortions and forms an unusual modulated phase that permeates the entire film [2,3]. Beyond about 20 ML, the modulated structure did not appear to evolve further and any excess Cu deposited was found to accumulate in islands of FCC material with poor epitaxial relationship to the film [4].

The X-ray diffraction measurements [3] suggested a model consisting of stripes of orthorhombic Cu with its enlarged lattice spacing directed alternately parallel and perpendicular to the surface. Interspersed between these stripes were filler regions of cubic (BCC) Cu that matched along  $\{1\ 1\ 0\}$  planes without dislocations. In BCC,  $\{1\ 1\ 0\}$  planes are the shear planes that are predominant in martensitic phases, so these are the obvious choice for domain boundaries. BCC metals tend to be “soft” to this shear mode; the two orthorhombic regions can be obtained by shearing the BCC structure along two opposing directions. All atoms in the model have full BCC 8-fold nearest-neighbor coordination. The model gave reasonably good agreement with the X-ray diffraction data, with each domain contributing a particular subset of the diffraction peaks seen [3].

A serious difficulty with the model arises when it is connected with the Au(1 0 0) substrate. Along the horizontal boundary, the Cu film is lattice matched *on average* with the substrate, but the orthorhombic distortions are so large that there would be horizontal mismatches larger than 1 Å at the interface. It is difficult to imagine distortions of the Au substrate this large are favorable. If, by contrast, it is postulated that the Cu–Au interface resembles the outer surface, for example by doubling the thickness of the film through a mirror operation about the bottom plane, the interfacial distortions would be entirely in the

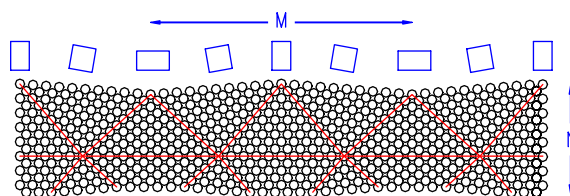


Fig. 1. Schematic model of the modulated film constructed without dislocations. Lines indicate the borders of homogeneous regions that join together with  $\{1\ 1\ 0\}$  planes.

vertical direction, but would also be in excess of 1 Å in magnitude. The amount of distortion needed in the model is known quite accurately because it is determined by the peak positions in the diffraction pattern [3].

An obvious compromise would be to construct the interface somewhere between these limits, as suggested in Fig. 1. This model of the interface keeps the distortions to about 0.5 Å by allowing them to coexist in both horizontal and vertical directions. There are still substantial unit-cell volume distortions needed for such an interface, but these could be accommodated by a pattern of intermixing of Cu and Au in the interfacial layer. It is clear from Fig. 1 that the geometry of the stripes results in an intimate connection between the *thickness* of the film and the *period* of modulation across the surface. Both of these quantities are well-defined experimental variables. The purpose of the present study aimed to explore the general validity of the proposed model by measuring the thickness dependence of the modulation period.

## 2. Experiment

Electroplating, in the bulk-deposition potential regime (beyond the first monolayer), is generally a rather crude way to control film thicknesses. During the measurement of the deposited film, the potential must not drift from a ‘safe’ range, where current does not flow to increase or decrease the thickness. The sample cannot be emerged from the electrolyte without losing potential control. In the previous studies on Cu/Au(1 0 0) a maximum

of 4 h of measurements were found to be possible [4]. The thickness could only be estimated by coulometry during the deposition and only rarely permitted reliable ‘topping-up’ of the coverage with subsequent depositions [4]. It was, therefore, impractical to undertake a systematic coverage-dependent structural study of the electrochemical Cu/Au(1 0 0) thin-film system.

In the present work we used vacuum deposition, whereby the coverage can be controlled reliably and reproducibly. The equilibrium state of the binary metallic system does not depend upon its original preparation, so electrochemical and vacuum deposition methods are expected to be analogous. Cu/Au films can be prepared at room temperature because interdiffusion is too slow to be relevant. Strictly the system is metastable and would intermix if annealed to form the intermetallic phases  $\text{Cu}_3\text{Au}$  and  $\text{CuAu}$ . A better choice for study is the Cu/Ag system which does not have the intermetallic phases; the solubilities of Ag in Cu and Cu in Ag are both  $<1\%$  [5]. Ag and Au have approximately the same lattice parameter and Au(1 0 0) and Ag(1 0 0) were, moreover, found to display the same progression of BCC and modulated structures upon Cu electrodeposition [4].

We, therefore, performed a UHV deposition experiment of Cu on Ag(1 0 0) at the X16A surface diffraction beamline at NSLS in a chamber with a base pressure of  $2 \times 10^{-10}$  Torr. The Ag(1 0 0) sample was electropolished before entering UHV then cleaned by cycles of sputtering and annealing. The deposition source was a graphite effusion cell held at  $1100^\circ\text{C}$ . The depositions were made with the sample at room temperature with a pressure of  $1 \times 10^{-9}$  Torr. X-rays from the NSLS bending magnet were focused with a toroidal mirror and monochromated with a double Si(1 1 1) monochromator selecting an energy of 10.6 keV. The diffraction signal was measured with a linear position sensitive detector behind  $2 \times 10 \text{ mm}^2$  slits 600 mm from the sample, which defined the resolution. A conventional tetragonal coordinate system was used for indexing the Ag substrate which redefines its (1 1 1) Bragg peak as  $(1 0 1)_{\text{tet}}$ . Two-dimensional scans were made in reciprocal space, parallel and perpendicular to the  $(1 0 L)_{\text{tet}}$  crystal truncation rod (CTR) which passes

through the  $(1 0 1)_{\text{tet}}$  Bragg peak of the Cu film and the  $(1 0 1)_{\text{tet}}$  substrate peak [6].

Below 10 ML, BCC Cu was found to grow in a layer-by-layer manner, as evidenced by dramatic temporal oscillations of the crystal truncation rods.  $(1 0 L)_{\text{tet}}$  rods were measured for  $L = 0.15$  to 0.92 and 1.08 to 2.08 using a calibrated attenuator for scans close to the (1 0 1) Bragg peak. Before fitting these data, they had to be corrected to account for certain experimental factors. A dead time correction had to be applied to account for the probability that an X-ray would arrive at the scintillation detector before the previous one had been processed, giving  $I = -\log(1 - I_{\text{obs}}\tau)/\tau$ , where  $I_{\text{obs}}$  is the measured rate and  $\tau = 1.8 \mu\text{s}$  is the dead time of our detector for a single pulse. This is reliable as long as  $I_{\text{obs}}\tau$  is significantly less than 0.3. Next a correction was applied to account for the geometry of the sample and the narrow slits which were used to define the incident beam and the detector acceptance. Only parts of the sample which were illuminated by the narrow incident beam and were in a line of site through the detector slits could contribute to the intensity measured at the detector. Finally, data taken with an attenuator were multiplied by a scaling factor.

The  $(1 0 L)_{\text{tet}}$  rod scans were then fit to a model where a variable number of layers of Cu was present on the Ag substrate. A surface roughness of  $\beta = 0.09$  was obtained by fitting the rod for clean Ag both above and below the  $(1 0 1)_{\text{tet}}$  Bragg peak. Truncation rods below the peak were then fit using  $\beta = 0.09$  and a Debye Waller factor of  $0.57 \text{ \AA}^2$ . The Cu was assumed to be commensurate with the Ag lattice in plane with a spacing of  $a = 2.89 \text{ \AA}$  and the out of plane lattice parameter  $c = 2.81 \text{ \AA}$  given by volume conservation. The only free parameters were the occupation of each Cu layer and the spacing between the Ag surface and the first Cu layer. Some occupation curves obtained through this fitting are shown in Fig. 2. The calculated occupations slightly over one may be due to the presence of Ag in the Cu as observed by Auger spectroscopy.

The layer occupations follow the sinusoidal variation with coverage seen for other systems. Ideal layer-by-layer growth would correspond to a

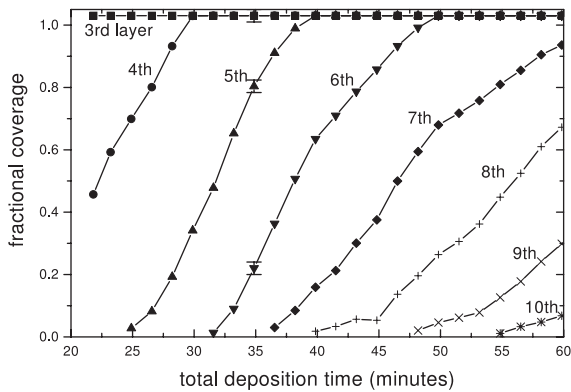


Fig. 2. Fractional coverage of Cu layers during deposition on Ag(100) surface. At 22 min 3 layers are fully occupied. Coverage was calculated by fitting crystal truncation rods. An estimation of the error is shown for the fit at 35 min.

diagonal line; the parabolic deviations indicate population of multiple layers simultaneously. The layer population curves become progressively broadened with deposition, indicating a roughening of the surface. The midpoints are nevertheless well defined and allow an accurate determination of the onset of modulation.

The broadened (101) peak of the BCC Cu film which appeared was found to be directly in line with the (101) of the Ag substrate, confirming the epitaxial nature of the film. Beyond 10 ML the film switched abruptly to the modulated structure as evidenced by the appearance of strong satellite diffraction features. These can be seen very clearly in the reciprocal-lattice map shown in Fig. 3. There are also satellites around the Ag substrate reflection, which was not measured, showing clearly that the substrate is also laterally modulated. This was seen in the earlier work on Cu/Au(100), but was ignored in the interpretation. For Cu/Au(100), the Au modulation satellites were much stronger than the Ag satellites seen here, in accordance with similar structure but higher  $Z$  of the substrate. Scans along other directions of reciprocal space showed a continuation of the same pattern, with two additional features: (i) some additional peaks with half-order satellite spacing; and (ii) some of the Cu peaks were split into double maxima

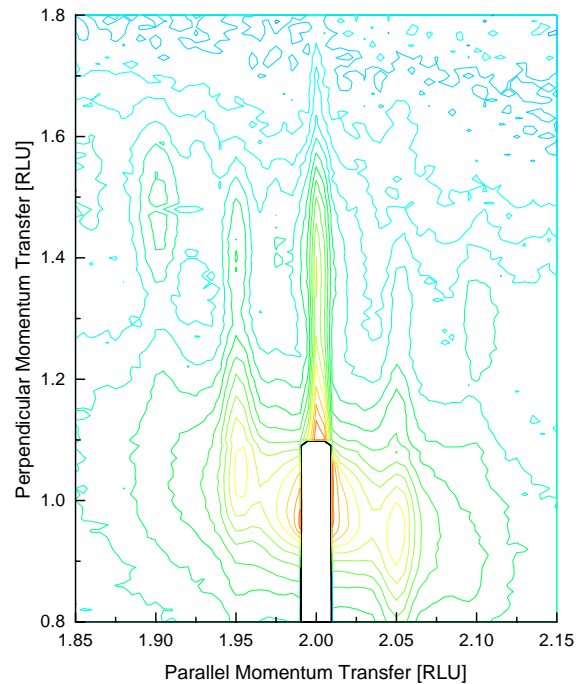


Fig. 3. Contour plot of the intensity distribution in the vicinity of the  $(101)_{\text{tet}}$  Bragg peak of a 15 ML Cu film grown on Ag(100). The reciprocal lattice units are those of Ag.

along the perpendicular direction. All these features will eventually have to be incorporated into a complete model of the structure of the modulated film.

To measure the evolution of the modulation period with film thickness, sequential scans were taken along the diagonal direction that passes through the five strongest peaks of the Cu diffraction pattern. Each 3 min scan corresponds to a deposit of about 1 ML. Some scans close to the onset of the modulations are shown in Fig. 4. The appearance of the modulation peaks is abrupt without any apparent precursor. There were usually five clear peaks—the CTR and four satellites—but occasionally two additional satellites could be distinguished. The experiment was repeated at different dose rates, as controlled by the effusion-cell temperature. The experiment was also repeated over a range of substrate temperatures between  $-37$  and  $149^\circ\text{C}$ .

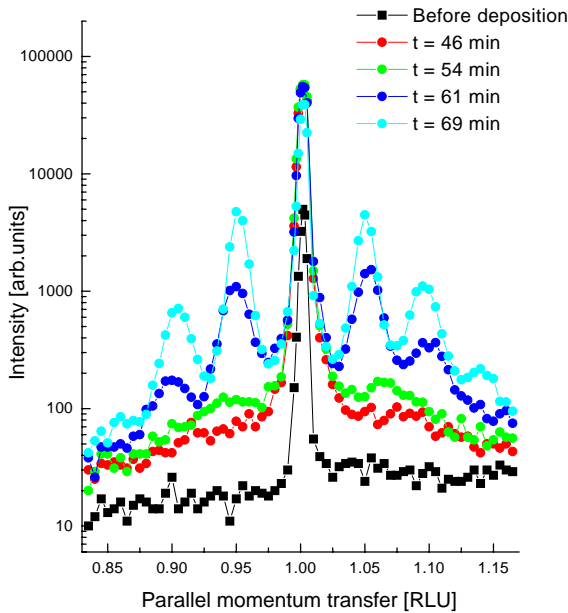


Fig. 4. Scans passing through the modulation peaks of a Cu film growing on Ag(100) during deposition. The abrupt onset of modulations can be seen. One curve shows a multi-Gaussian fit used to extract the peak positions.

### 3. Discussion

It was possible to fit a multi-Gaussian line shape to determine the peak positions in the diagonal scans. The peak separations,  $\Delta h$ , were calculated and used to determine the modulation period, measured in lattice spacings, denoted  $M$  in Fig. 1, according to  $M = 1/\Delta h$ . Four separate determinations of the  $M$  are plotted in Fig. 5 as a function of coverage during the deposition, denoted  $N$  in Fig. 1. Defining the parameters this way  $N$  is measured in monolayers and  $M$  in unit cells, meaning that the  $M$  spacing is twice as great as the  $N$  spacing. We used an *internal* calibration of the coverage  $N$ , assuming it increased linearly in time after opening the shutter of the effusion cell, and assuming the abrupt onset of the modulations occurred at exactly 10 ML. It can be seen that there is a continuous trend with coverage once the instability sets in at 10 ML. This trend is explained fairly well by the straight line marked  $M = N + 9$ , according to the equation used to fit the data empirically.

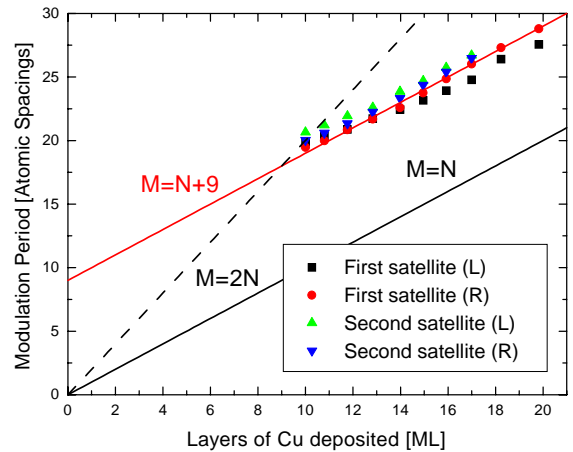


Fig. 5. Modulation period (in unit-cell spacings) observed during deposition. Multiple measurement appertain to the different satellite reflections. Straight lines correspond to models discussed in the text.

As shown in Fig. 1, an  $M = N + 9$  model suggests that the changes in structure penetrate into the substrate, which is confirmed by the presence of satellite peaks around the Ag Bragg peaks, as in Fig. 3. It is possible to explain the observed thickness trend as resulting from the thickness evolution of the alternating orthorhombic domains. If we define  $a$  as the atomic spacing in the direction of the domain stripes and  $c$  as the out of plane atomic spacing, the model can be seen to have spatial domains which sequence through  $a > c$ ,  $a = c$  and  $a < c$  as shown by the carton boxes in Fig. 1.

The basic domain model of the modulated film structure in Fig. 1 was based on a previous analysis of a single film thickness. The scaling of the structure with thickness, measured here, allows further details to be unraveled. Fig. 6 shows schematically four variants of the model in which the domain structure might evolve with thickness. All the variants are based on joining slabs of orthorhombically distorted BCC to undistorted BCC along  $\{110\}$  planes, which are inclined at  $\sim 45^\circ$  to the interface. As mentioned above, this is the “soft” direction of the BCC lattice in which shear can be accommodated. The strain directions of the orthorhombically distorted stripes alternate between in-plane and out-of-plane to produce the



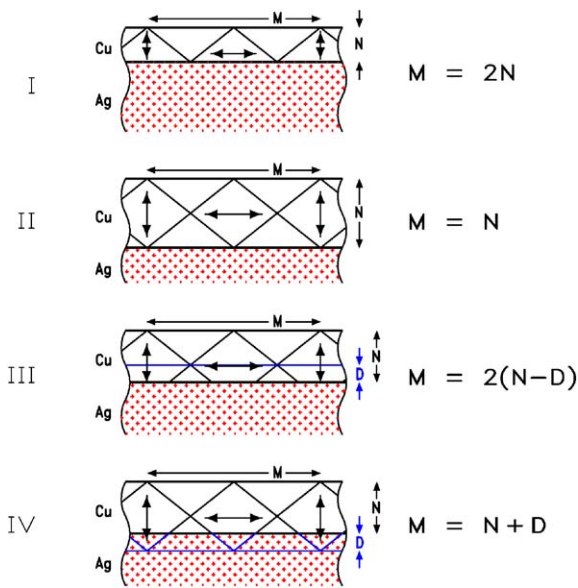


Fig. 6. Schematic models of the domain architecture of the films that lead to different predictions for the evolution of the modulation period with thickness.

modulation, yet maintain the same average lattice parameter to avoid dislocations at the interface with the substrate. The variants are all distinguishable by the scaling relationship of  $M$  with  $N$ .

Variant I has the orthorhombic domains fully in contact with the substrate. The  $\sim 45^\circ$  inclination of the domain boundaries assures the scaling relation  $M = 2N$  by simple geometry. As discussed above, this leads to unrealistically large displacements parallel to the interface that would elastically deform the substrate. Variant II has the orthorhombic domains completely surrounded by cubic domains, symmetrically placed on both sides of the film. This now has large perpendicular displacement to be accommodated by strain in the substrate. It also has a different scaling relation,  $M = N$ .

Variants III and IV correspond to the same film structure which is intermediate between the first two: it has a mixed interface with both cubic and orthorhombic domains in contact with the substrate. This is desirable because it generates both parallel and perpendicular displacements in the substrate, but with a smaller magnitude than before. The picture in Fig. 6 suggests equal areas

of cubic and orthorhombic domains by placing the interface halfway between the extremes of variants I and II. Variants III and IV are different in whether it is the size of the cubic or the orthorhombic domains that changes when the film thickens; again these are extreme limits of the intermediate model. The third variant conserves the size of the *cubic* domains to a constant thickness  $D$  (or a length  $2D$  along the interface). This scales as  $M = 2(N - D)$ . In the opposite extreme, the final variant conserves the lateral size of the *orthorhombic* domains. This is modeled by considering the domains to extend to an imaginary constant depth  $D$  below the interface, which leads to a scaling rule  $M = N + D$ .

Thus, the four variations of the model all predict different scaling rules. When  $M$  scales with coverage as  $2N$ , a single layer of domains is implicated; when  $M \propto N$ , we need a double layer of domains. The offset  $D$  adjusts for the termination at a mixed interface. Since we observe  $M = N + 9$  experimentally, we favor variant IV with  $D = 9$ .  $D = 9$  may also explain why the modulated film only appears beyond  $N = 10$ , since  $D \leq N$  is required for the establishment of the cubic domains at the interface.  $D = 9$  implies a fixed length (18 unit cells) of interface between the orthorhombic domains and the substrate, which might adopt some specific structure, perhaps with Cu/Ag intermixing. When the film thickens beyond  $N = 10$ , the expansion of the modulation period,  $M$ , is accommodated by lateral growth of the cubic domains at the interface.

We thank J.X. Wang for electropolishing the Ag substrate. The experiments were carried out at Beamline X16A of the National Synchrotron Light Source (NSLS), which is supported under DOE Contracts DEAC02-98CH10886 and DEFG02-91ER45439. The research was supported by the National Science Foundation under Contract DMR 03-08660.

## References

- [1] J.W. Matthews, A.E. Blakeslee, J. Cryst. Growth 27 (1974) 118.

- [2] R.J. Randler, D.M. Kolb, B.M. Ocko, I.K. Robinson, *Surf. Sci.* 447 (2000) 187.
- [3] B.M. Ocko, I.K. Robinson, M. Weinert, R.J. Randler, D.M. Kolb, *Phys. Rev. Lett.* 83 (1999) 780.
- [4] R.J. Randler, personal communication.
- [5] T.B. Massalski (Ed.), *Binary Alloy Phase Diagrams*, second ed., vol. 1, ASM International, 1990.
- [6] I.K. Robinson, D.J. Tweet, *Rep. Prog. Phys.* 55 (1992) 599.